Evaluation of isomorphous models of alloys

J. S. Faulkner and N. Y. Moghadam
Alloy Research Center and Department of Physics, Florida Atlantic University, Boca Raton, Florida 33431

Yang Wang
Pittsburgh Supercomputing Center, Pittsburgh, Pennsylvania 15213

G. M. Stocks
Metals and Ceramics Division, Oak Ridge National Laboratory, Oak Ridge, Tennessee 37830
(Received 3 July 1997)

Order-*N* methods for calculating the electronic structure of clusters containing hundreds of atoms using realistic self-consistent density-functional theory local-density approximation potentials make it possible to test alloy theories more definitively. Tests are carried out on isomorphous models of alloys in which the atoms of each species are treated as identical. In contrast, the order-*N* calculations lead to a polymorphous model in which all of the atoms are unique. Isomorphous models are seen to reproduce average densities of states and cohesive energies surprisingly well, in spite of their deficiencies in other areas. [S0163-1829(98)06913-6]

I. INTRODUCTION

Efforts have been made for many years to understand the electronic structure of substitutional solid-solution alloys, which are called terminal solid solutions in the metallurgical literature. This is a difficult problem because the lack of long-range order means that Bloch's theorem does not hold, and band-theory methods for calculating the electronic structure are not applicable. When digital computers came into more general use in physics research, simple one-dimensional models[1] and three-dimensional models[2] of alloys were used to elucidate the general features of the electronic structure. It was learned that highly reproducible characterizations of the electronic states can be obtained from a single calculation if the number of atoms in the model is large enough so that the properties being calculated are self-averaging.[3] Today, order-*N* methods for density-functional theory local-density approximation (DFT-LDA) (Ref. 4) calculations of the electronic structure for clusters of hundreds or thousands of atoms make it possible to test alloy theories more definitively on realistic three-dimensional systems that can also be studied experimentally. They also make it possible to study the additional theoretical questions that arise in the process of iterating the DFT-LDA potentials to self-consistency. They require supercomputers, preferably with parallel architecture, and would have been impractical a short time ago.

For the sake of being definite, a disordered alloy will be pictured as an infinite collection of two kinds of atoms, A and B, placed on the sites of a Bravais lattice with probabilities equal to their concentrations, c and $1-c$. Experimentally, materials can be fabricated that approximate this ideal picture by quenching certain binary metallic alloys from high temperatures. If the Warren-Cowley short-range order coefficients α_{lmn} obtained from diffuse scattering intensities of x rays or neutrons are small, the sample may be treated as disordered for most purposes. It might be thought that the placement of the atoms precisely on the sites of the average lattice is a significant approximation. One of the striking results from x-ray and neutron-diffraction experiments on solid solutions is the sharpness of their Bragg peaks. Analysis of the experimental Debye-Waller factor shows[5] that the rms displacement of atoms from their average position caused by the size effect is less than one-third the thermal displacement at room temperature, even for alloys with large size differences.[6] This conclusion is borne out by the more sophisticated experimental studies of atomic size effects with the 3λ method[7,8] that make use of x rays generated by a synchrotron.

The alloy models used in the earlier computational studies[1,2] were chosen to be isomorphous, which means that the potential functions used on all of the A sites are the same, as are those on the B sites. The calculations show that the theories that had been proposed, the rigid-band model[9] and virtual-crystal approximation,[10] could only be used for alloys in which neither of the constituent atoms is a strong scatterer of conduction electrons. This eliminates many metallic alloys of technological importance because they contain transition metals. Efforts to treat strong scattering led first to the average t-matrix approximation,[11] and later to the coherent potential approximation (CPA).[12] All of the theories that have been mentioned have the effect of replacing the different scatterers in the alloy with a single effective scatterer so that, for the purposes of a calculation, the disordered system is replaced by an ordered one. The most generally successful theory is the CPA. It has been used to explain a wide range of experiments on metallic alloys,[13] and it contains the rigid-band model, the virtual-crystal approximation, and the average t-matrix approximation as limits when the parameters of the alloy are such that those theories should be applicable.

In Sec. II, various versions of the CPA are discussed. In Sec. III, the locally self-consistent multiple scattering method used for order-*N* calculations is described briefly, and the results of calculations on realistic models of alloys are compared with the predictions of some isomorphous

CPA's. The results of this comparison are discussed in Sec. IV.

II. COHERENT POTENTIAL APPROXIMATIONS

The remarkable insight that led to the first CPA theory evolved over a period of time with contributions from many scientists, but it was first clearly formulated in Ref. 12 in terms of the isomorphous models that were in use in the computational studies. The electron interactions with all the A atoms in the alloy were assumed to be described by the same one-electron potential $\nu_A(\mathbf{r})$, and interactions with the B atoms are represented by $\nu_B(\mathbf{r})$. The procedure for finding the effective CPA potential $\hat{\nu}(\mathbf{r})$ starts with the calculation of the scattering matrix that describes scattering from $\nu_A(\mathbf{r})$ embedded in a lattice, with $\hat{\nu}(\mathbf{r})$ on all the other lattice sites, $\tau_A(E)$. The scattering matrix $\tau_B(E)$ is obtained similarly. The CPA relation that defines the $\hat{\nu}(\mathbf{r})$ is

$$c\,\tau_A(E)+(1-c)\,\tau_B(E)=0, \tag{1}$$

which means that, on the average, the effective medium is such that there is no scattering from an A or B atom embedded in it. It follows that $\hat{\nu}(\mathbf{r})$ depends on the energy E and the concentration c, and it turns out to be complex. As this approximation was studied by others, it came to be understood that it could be described in terms of an infinite sum of certain classes of terms in perturbation theory which could be represented by diagrams.[14] The result that the effective potential $\hat{\nu}(\mathbf{r})$ is complex is a significant achievement of this theory, because it represents correctly the fact that propagators in random alloys are damped. Later additions to the theory included a more clear prescription for calculating the properties of the alloy from the CPA Green's function for the general case of muffin-tin potentials in three dimensions.[15]

As the CPA began to be used to calculate the electronic structure of real alloys to explain experimental measurements, it became desirable to have a method for calculating $\nu_A(\mathbf{r})$ and $\nu_B(\mathbf{r})$ self-consistently using the DFT-LDA. A scheme was proposed to do this that seemed to work well in applications,[16] and was later generalized to calculate total energies.[17] This self-consistent-field method is called the Korringa-Kohn-Rostoker (KKR)-CPA.[18]

The KKR-CPA was criticized for not treating the Coulomb energy correctly, and a simple model was proposed for predicting the charge on an atom in an alloy.[19,20] A method for including a more explicit contribution from the Coulomb energy in the CPA, while retaining the isomorphous model of the alloy, was developed.[21] It is based on the assumption that the charge on an atom in the alloy would be screened by its nearest neighbors, just as it is for impurities in otherwise perfect metals. This screening assumption is also used as the basis for a more complicated theory for improving the treatment of the Coulomb energy called the charge-correlated CPA (cc-CPA).[22] By making further simplifications, the cc-CPA was transformed into an isomorphous CPA that differs from the one suggested in Ref. 21 by the choice of a prefactor.[23] We will refer to these two isomorphous CPA's as the screened CPA (SCPA).

Self-consistent DFT-LDA calculations on supercells containing hundreds of atoms have been carried out with the order-N method that will be described in Sec. III, and these are the basis for extensive investigations of the Coulomb energy in alloys.[24–26] Calculations on a Cu-Zn alloy with a 1024-atom supercell show[26] that it is necessary to sum the contributions from a very large number of nearest-neighbor shells in order to obtain the correct value for the Coulomb potential at any specific site, but the average of the Coulomb potentials at the Cu sites or at the Zn sites alloy is short range. This result can be used as a justification for the screening assumption in the SCPA of Refs. 21 and 22, although the original belief that the origin of the Coulomb potential in alloys is qualitatively similar to that in the impurity problem is clearly not true.

The order-N calculations lead to a polymorphous model of the alloy, in which every atom is seen to be unique. Even if two atoms are of the same species, their charge densities are different because their environments are different, as will be demonstrated numerically in Sec. III. It follows that the A or B atomic potentials, $\nu_{A,i}(\mathbf{r})$ and $\nu_{B,i}(\mathbf{r})$, depend on the site index i. This conclusion was discussed at great length in Ref. 26.

For a model of an alloy with a specified distribution of atoms on the sites of the Bravais lattice, it is possible to define a polymorphous CPA in which the scattering matrix $\tau_{A,i}(E)$ describes the scattering from $\nu_{A,i}(\mathbf{r})$ embedded in a lattice with $\hat{\nu}(\mathbf{r})$ on all the other lattice sites. The CPA condition becomes

$$\sum_{i\subset A}^{N_A}\tau_{A,i}(E)+\sum_{i\subset B}^{N_B}\tau_{B,i}(E)=0, \tag{2}$$

where N_A and N_B are the number of A and B atoms in the crystal. This is still a CPA approximation because the disordered alloy will be replaced by an ordered system with the effective potential $\hat{\nu}(\mathbf{r})$ on every site. The potential $\hat{\nu}(\mathbf{r})$ is a complex function of E and c, and it can be used to define a Green's function and a Bloch spectral density function as for isomorphous CPA's. Of course, further approximations have to be made in the implementation of the theory because there are an infinite number of terms in the sums. In particular, calculations are carried out with supercells containing a finite number of atoms. Such a polymorphous CPA has been proposed and investigated.[27] The comparison of the predictions in Sec. III of two isomorphous CPA's with order-N calculations leads to the conclusion that there is some room for improvement in such theories.

III. ORDER-N CALCULATIONS

The order-N method used in the following calculations is called the locally self-consistent multiple scattering (LSMS) method, and a complete description of it is in the literature.[28,29] It is based on the multiple-scattering equations of Rayleigh[30] that are also the basis for the Korringa-Kohn-Rostoker method.[31] It has been demonstrated that the method is well adapted to treat transition metals. When solving the multiple-scattering problem, the interaction of an atom with all neighbors in a local interaction zone that includes four or more nearest-neighbor shells is treated exactly. The Coulomb interactions with the remaining infinity of atoms are also treated exactly, but the multiple-scattering part is approximated. This process is repeated for each of the N atoms

in the cell, and the entire process is iterated until self-consistency is attained. The calculations are speeded up by exploiting the analytic properties of the single-particle Green's function and the variational properties of the DFT-LDA, but they would be rather time consuming without a massively parallel supercomputer.

The LSMS method is used here to carry out DFT-LDA self-consistent calculations on models of fcc and bcc copper-zinc alloys. This alloy system was chosen because it is the classic example of a Hume-Rothery alloy,[32] and has been discussed extensively in the materials science literature. Since the constituents are both transition metals, experience from ordinary band-theory calculations leads us to expect that the muffin-tin approximation that we use will not introduce significant errors. Finally, there is no experimental reason to believe that the size difference between copper and zinc would cause the rms deviation of the atomic positions from the sites of the ideal lattice to be significant.[5]

The atoms in a given supercell are distributed randomly on the lattice sites with probabilities c and $1-c$. The supercells are then periodically reproduced to fill all space. Alloys containing 10%, 25%, 50%, 75%, and 90% of copper are considered, and calculations are also done for the pure metals. All of these calculations are done for both the fcc and bcc phases. For the fcc alloys, 500 atoms are randomly distributed on the ideal lattice positions in the supercell, and the lattice constant of 6.90-bohr radii is used for all concentrations. For the bcc case, 432 atoms are used, and the lattice constant for all concentrations is chosen to be 5.50-bohr radii. Warren-Cowley short-range order parameters are calculated for the first 12 nearest-neighbor shells, and they are of the order of 0.01. Experimentally, alloys with sro parameters ten times as large are observed to behave like random alloys. Tests are made to demonstrate that the samples are large enough so that the calculations on these alloy models give a realistic picture of the properties of the infinite alloys. These tests, and the other assertions that have been made about these alloy models, were discussed at great length in Ref. 26. A careful definition of the concept of the charge to be associated with a site is also given in that reference, where the relation between these charges and the Coulomb potentials at each site is demonstrated.

In all of the LSMS calculations, the number of different charges found on the copper or zinc atoms is equal to the number of such atoms in the sample. The statistical distribution of these charges is shown in Fig. 1 for 50% fcc and bcc alloys. The standard deviation is approximately 25% of the average charge for each atom in the fcc and bcc alloys. Clearly, the assumption in isomorphous models that every copper or zinc atom has the same charge is not realistic.

The LSMS calculations produce a set of self-consistent potentials $\nu_{A,i}(\mathbf{r})$ and $\nu_{B,i}(\mathbf{r})$ for each atom in the sample. They contain all of the Coulomb effects that can be obtained from a DFT-LDA calculation. The average of these potentials over all the atoms of each species will lead to potentials $\overline{\nu_A}(\mathbf{r})$ and $\overline{\nu_B}(\mathbf{r})$ that can be used in an isomorphous CPA, which is called the LSMS-CPA. Since the self-consistency steps involved in generating the average potentials, including the Madelung potentials, are in the LSMS calculation, it would not be proper to iterate the $\overline{\nu_A}(\mathbf{r})$ and $\overline{\nu_B}(\mathbf{r})$ further in the LSMS-CPA.

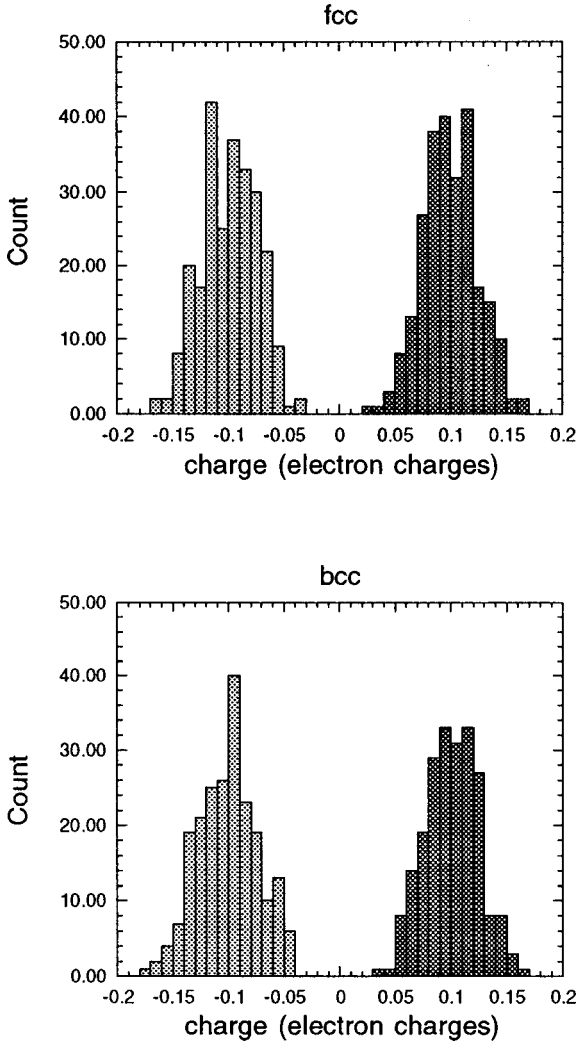

FIG. 1. A histogram distribution showing the charges on the sites of two 50% copper-zinc disordered alloys. The charges with positive sign correspond to copper atoms, which gain electronic charge in the alloy. The negative charges are associated with the zinc atoms. The upper panel is for models of fcc alloys with $a=6.90$ a.u. calculated with supercells that contain 500 atoms, and the lower panel is for bcc alloys with $a=5.50$ a.u. and 432 atoms.

The average charge on a site $\langle q\rangle_A$ or $\langle q\rangle_B$, calculated by any of the available methods, is an approximately linear function of concentration, so the charge transfer depends only weakly on c. In Fig. 2, LSMS-CPA calculations of $\Delta=\langle q\rangle_{Cu}-\langle q\rangle_{Zn}$ for the fcc and bcc Cu-Zn alloys described above are compared with the average charge transfers taken directly from the LSMS data. The fact that the charge transfers are very nearly the same is not a great surprise, although it is not required and seems to imply that the underlying CPA idea is a powerful one. Charge transfers calculated with potentials obtained with the self-consistent KKR-CPA method[16] are also shown in Fig. 2. This charge transfer is about 70% of the one predicted by the LSMS, for both the fcc and bcc alloys. From Fig. 2 one can obtain the impression that LSMS-CPA calculations are almost as good as LSMS calculations, and that KKR-CPA calculations are only 70% as good, but the story is not so simple.

Since the average potentials $\overline{\nu_A}(\mathbf{r})$ and $\overline{\nu_B}(\mathbf{r})$ contain all of the Coulomb effects, the LSMS-CPA will achieve the

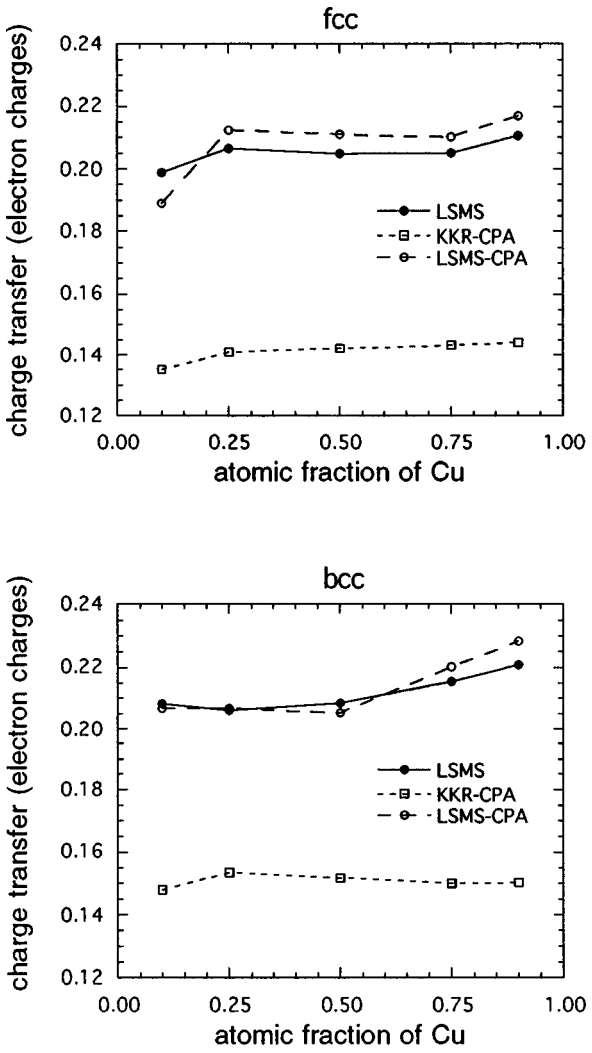

FIG. 2. The difference in the average charge of the copper atoms and zinc atoms on the sites of copper-zinc disordered alloys as a function of concentration. The charge transfers calculated with the LSMS method are shown by the dots connected with a solid line. The circles connected with a dashed line show the charge transfers calculated with the LSMS-CPA, and the KKR-CPA results are shown by the boxes connected with a short-dashed line. The upper panel is for models of fcc alloys with $a=6.90$ a.u. calculated with supercells that contain 500 atoms, and the lower panel is for bcc alloys with $a=5.50$ a.u. and 432 atoms.

same ends as the SCPA, except that no assumption is made about the screening length for the Coulomb potential in the alloy. We do not claim that LSMS-CPA calculations are the same as SCPA calculations, but we do claim that they provide a test of the improvement on KKR-CPA calculations that can be expected by including Coulomb effects in an isomorphous model of the alloy. In particular, the charge transfer Δ obtained from the SCPA should be comparable with the one from the LSMS-CPA. A comparison with available SCPA energy of mixing calculations will be shown in Sec. IV.

Cohesive energy calculations were carried out for all the Cu-Zn alloys and for the pure materials in the fcc and bcc phases. The free energy of mixing is defined as

$$\Delta E_{\mathrm{mix}}=E_{\mathrm{alloy}}-cE_{\mathrm{Cu}}-(1-c)E_{\mathrm{Zn}}. \tag{3}$$

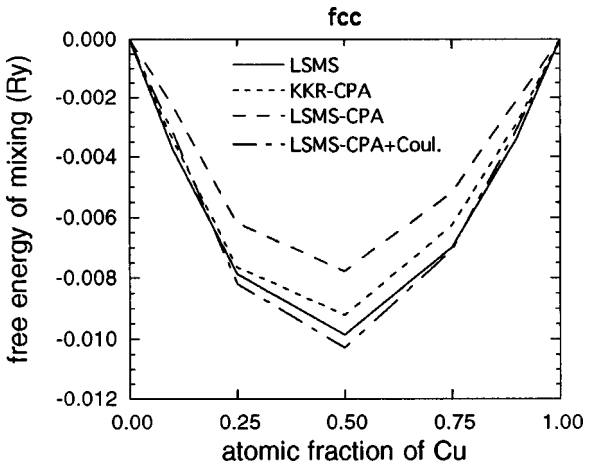

FIG. 3. The free energies of mixing of five fcc copper-zinc disordered alloys with $a=6.90$ a.u. as a function of concentration. The results of the LSMS calculations with supercells that contain 500 atoms are shown by the solid line. The KKR-CPA and LSMS-CPA give to the values shown by the dashed line and the line made up of short dashes. Adding the bare interatomic Coulomb energies to these values leads to the results shown by the line made up of long and short dashes.

It can be seen from Fig. 3 that, for the fcc alloys, the ΔE_{mix} for both of the isomorphous CPA's are remarkably close to the LSMS results. The values for the KKR-CPA agree better than those for the LSMS-CPA, but the latter can be improved. The contribution to the LSMS cohesive energy from the interatomic Coulomb interactions U^C was calculated for these same alloy models in Ref. 26. ΔE_{mix}, obtained by adding U^C to the ΔE_{mix} calculated with the LSMS, is also shown in Fig. 3. In a similar fashion, an approximation to U^C is added to the mixing energies from the CPA step in the SCPA calculations of Refs. 21 and 22. For the 50% alloy, the LSMS-CPA$+U^C$ binding differs from the LSMS value by about the same amount as the LSMS-CPA binding, but the LSMS-CPA$+U^C$ overbinds while the LSMS-CPA underbinds.

The results are qualitatively the same for bcc alloys, as can be seen from Fig. 4. The overbinding of the LSMS-CPA$+U^C$ is greater for this case than the underbinding for the LSMS-CPA. Also, there is an asymmetry in the energy of mixing calculated with the isomorphous CPA's that does not appear in the LSMS energy. When this result was observed, the LSMS calculations were rerun with different samples and the local interaction zones were made larger, but no significant change was observed.

Another quantity of considerable interest in the theory of alloys is the electronic density of states (DOS), defined so that $n(E)dE$ is the number of eigenvalues between E and $E+dE$. The average DOS on the copper and zinc sites are called $n_{\mathrm{Cu}}(E)$ and $n_{\mathrm{Zn}}(E)$, and the DOS for the alloy is $n(E)=cn_{\mathrm{Cu}}(E)+(1-c)n_{\mathrm{Zn}}(E)$. In the LSMS calculations, every copper and zinc site in an alloy has a different DOS, and these must be averaged in order to find the $n_{\mathrm{Cu}}(E)$ and $n_{\mathrm{Zn}}(E)$ from that calculation. The isomorphous CPA's give only one $n_{\mathrm{Cu}}(E)$ and $n_{\mathrm{Zn}}(E)$ for each alloy. The $n_{\mathrm{Cu}}(E)$ and $n_{\mathrm{Zn}}(E)$ calculated with the LSMS-CPA are compared in Fig. 5 with the average DOS from the LSMS calculations for the 50% fcc and bcc alloys. The LSMS-CPA $n_{\mathrm{Cu}}(E)$ and $n_{\mathrm{Zn}}(E)$

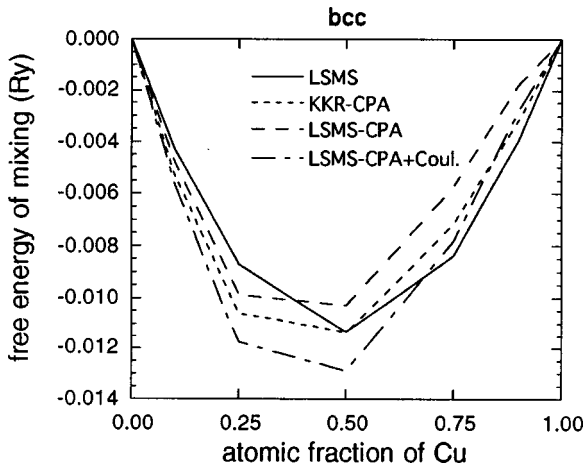

FIG. 4. The free energies of mixing of five bcc copper-zinc disordered alloys with $a=5.50$ a.u. as a function of concentration. The results of the LSMS calculations with supercells that contain 432 atoms are shown by the solid line. The KKR-CPA and LSMS-CPA give the values shown by the dashed line and the line made up of short dashes. Adding the bare interatomic Coulomb energies to these values leads to the results shown by the line made up of long and short dashes.

for the bcc alloy show a pronounced two-peak structure in the d-band region that is well known from band-theory calculations. The average $n_{\mathrm{Cu}}(E)$ from the LSMS calculations is quite similar to the LSMS-CPA $n_{\mathrm{Cu}}(E)$. $n_{\mathrm{Zn}}(E)$ does not show the two-peaked structure, however.

$n_{\mathrm{Cu}}(E)$ and $n_{\mathrm{Zn}}(E)$ calculated with the LSMS-CPA and the KKR-CPA are compared in Fig. 6 for the 50% fcc and bcc alloys. At first sight, the difference between these curves seems quite small, given the fact that the charge transfer predicted by the KKR-CPA is only 70% of the correct value. However, the slight upward shift of the copper d bands and the slight downward shift of the zinc d bands in the KKR-CPA calculations is quite enough to account for that error, because there are ten electrons in the d bands. A conclusion that can be drawn from the data in Figs. 5 and 6 is that the isomorphous CPA's lead to remarkably good predictions for the densities of states of alloys.

All of the calculations on fcc alloys described above were carried out for a lattice constant $a=6.90$ bohr radii, while the bcc alloys have $a=5.50$ bohr radii. This makes it easier to compare the parameters calculated for different concentrations, but it leads to an error in the lattice constant of $\pm 4\%$ at the ends of the concentration range that will have a significant effect on the free energies of mixing. It is of interest to apply the same analysis to a model that should be comparable with experiment, so additional LSMS calculations in which the lattice constants are adjusted to minimize the cohesive energies were carried out for a series of fcc alloys. Cohesive energy calculations were performed for pure copper and zinc and for alloys containing 10%, 25%, 50%, 75%, and 90% of copper using supercells that contain 256 atoms. It was found that doubling the size of the supercells changes the cohesive energy by a few micro-Rydbergs. The equilibrium lattice constants that result from these calculations are compared with experiment and with the results of other DFT-LDA calculations[33] in Fig. 7. As usual, the DFT-LDA lattice constants are slightly smaller than experiment, partly

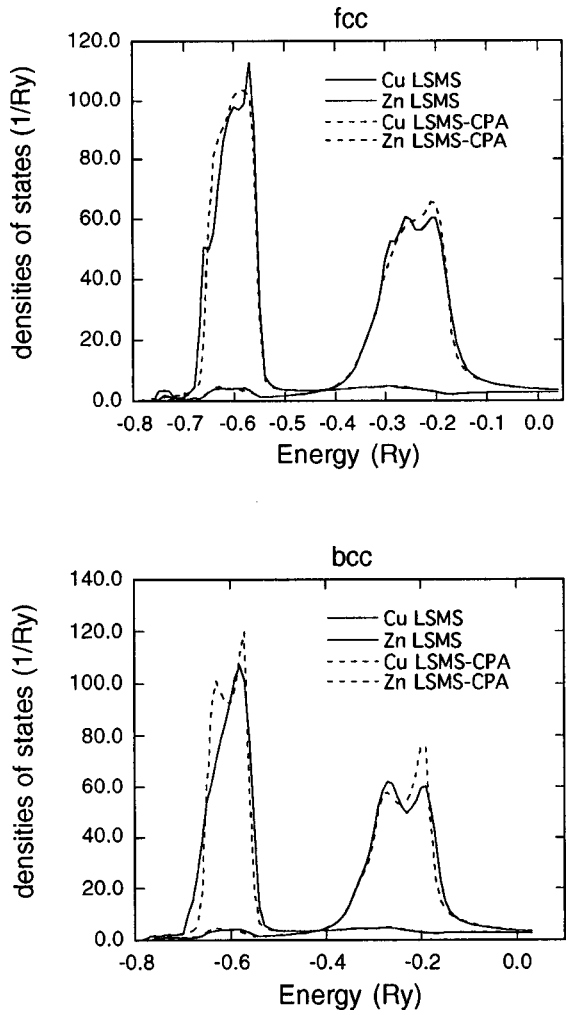

FIG. 5. The densities of states $n_{\mathrm{Cu}}(E)$ and $n_{\mathrm{Zn}}(E)$ for 50% copper-zinc disordered alloys. The solid curves show the DOS calculated with the LSMS, and the dotted curves are that obtained with the LSMS-CPA. The upper panel is for a model of a fcc alloy with $a=6.90$ a.u. calculated with a supercell that contains 500 atoms, and the lower panel is for a bcc alloy with $a=5.50$ a.u. and 432 atoms. The energy is relative to the Fermi energy.

because of zero point motion and thermal expansion. The shape of the curve agrees with experiment,[34] however. Of course, the fcc phase only exists in nature for alloys that contain more than 60% copper.

The cohesive energy calculations described above were used to obtain the free energies of mixing for the fcc alloys with the lattice constants shown in Fig. 7. They are compared in Fig. 8 with LSMS-CPA and KKR-CPA energies, also carried out on alloys with the proper lattice constants. The experimental energies of mixing for the α-phase fcc alloys are also shown.[35] The predictions of the isomorphous CPA's agree very well with those of the LSMS calculations; but the free energies of mixing obtained from experiment are larger than the LSMS predictions. A possible explanation for this was touched on in Ref. 29. The alloy models that have been discussed on this point were constructed with a random number generator, and were checked for randomness. It is quite easy to build any degree of short-range order into a sample, and the LSMS calculations are no more difficult for that case. Calculations were carried out[29,36] on a random

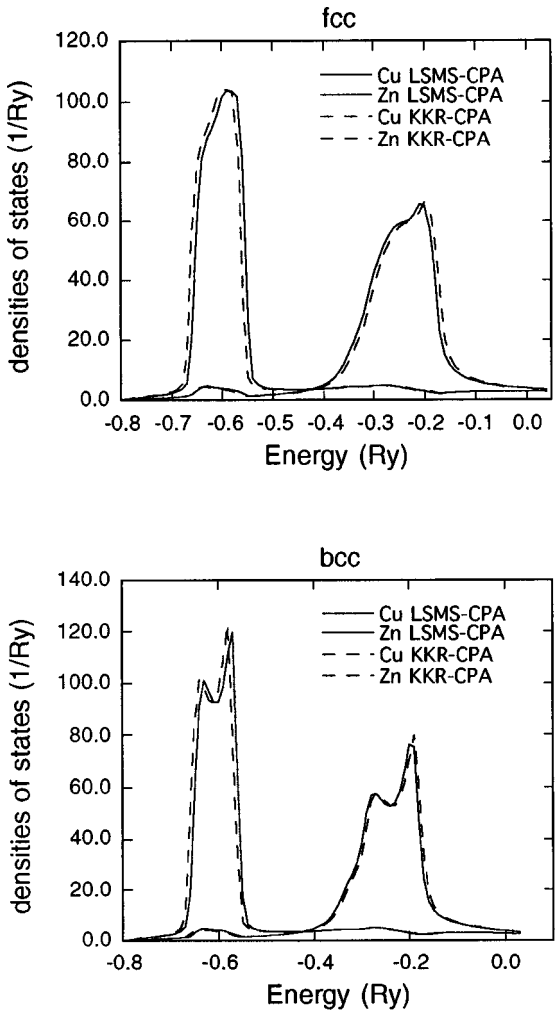

FIG. 6. The densities of states $n_{\mathrm{Cu}}(E)$ and $n_{\mathrm{Zn}}(E)$ for a model of a 50% fcc copper-zinc disordered alloy with $a=6.90$ a.u. The solid curves show the DOS calculated with the LSMS-CPA, and the dotted curves are those obtained with the KKR-CPA. The energy is relative to the Fermi energy.

sample of a 30% fcc alloy made up of 256 atoms, and on a model that has the experimentally observed Warren-Cowley short-range order coefficients.[37] The energy of the alloy with short-range order is found to be lower by 1.17-mRy/atom. Assuming that short-range order (SRO) would lower the free energies of mixing of all the alloys by a comparable amount, we change the LSMS free energies of mixing by $\Delta E_{\mathrm{SRO}}=-5.77c(1-c)$mRy/atom, where c is the atomic fraction of copper in the alloy. This estimated curve is shown in Fig. 8, and is seen to agree with the experimental free energies of mixing within the concentration range of copper-rich primary solid solutions.

It might seem at first glance that the agreement of the predictions of the LSMS-CPA$+U^C$ with experiment is very good. In fact, that agreement must be considered fortuitous, because the best values for ΔE_{mix} that can be obtained for this model from the DFT-LDA are the ones from the LSMS calculations. The overbinding predicted by these LSMS-CPA$+U^C$ calculations was also seen in Figs. 3 and 4.

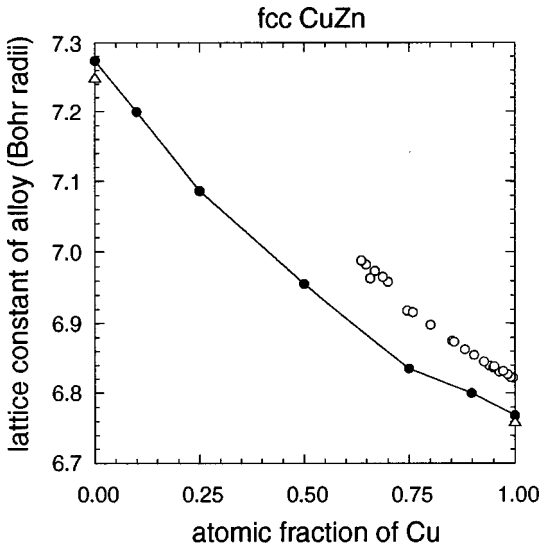

FIG. 7. The dots connected with the line indicate the lattice constants calculated for fcc copper and zinc and for models of 10%, 25%, 50%, 75%, and 90% fcc copper-zinc alloys. The calculations are done with supercells that contain 256 atoms. The open circles are the experimental data (Ref. 34). The triangles are the calculated values of Ref. 33.

IV. DISCUSSION

It is possible that theorists would have been reluctant to invest the effort that it took to develop the isomorphous CPA theory for alloys if they had seen the width of the distribution of charges shown in Fig. 1. That would be unfortunate, be-

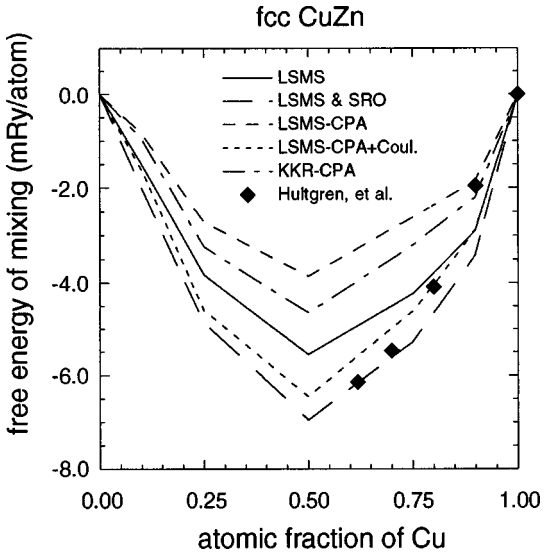

FIG. 8. The energy of mixing calculated with the order-N LSMS method for no short-range order (solid line) and an estimate of the experimental short-range order (the line with long dashes). The calculations were carried out for fcc copper and zinc and for models of 10%, 25%, 50%, 75%, and 90% fcc copper-zinc alloys with supercells that contain 256 atoms. The lattice constants used are shown in Fig. 7. The LSMS-CPA and KKR-CPA energies of mixing are shown with the long dashed line and the long-and-short-dashed line. The LSMS-CPA plus the interatomic Coulomb energy U^C is shown with the dashed line. The experimental energies of mixing from Ref. 35 are shown by the diamond-shaped marks.

cause the comparisons in Figs. 3–6 and also Fig. 8 show that the predictions of densities of states and energies of mixing obtained from isomorphous CPA are remarkably good. This is not unexpected because many experiments on alloys have been successfully explained using this theory. The physical pictures that have come from the theory, such as the existence of a Fermi surface with varying degrees of smearing, are useful and correct.

The KKR-CPA gives a value for the charge transfer in Cu-Zn alloys that is only 70% of the LSMS result, while the LSMS-CPA gives a value that is almost the same as the LSMS. In spite of this, the magnitude of the difference between the energy of mixing given by these CPA's and the LSMS calculation is almost the same, and is quite small. In the calculations on Cu-Zn alloys with realistic lattice constants in Fig. 8, the KKR-CPA underbinds by about 1 mRy, while the LSMS-CPA$+U^C$ overbinds by approximately the same amount.

$\Delta E_{\rm mix}$ for fcc Cu-Zn alloys has been used as a test case for other calculations using the KKR-CPA,[17] as well as more recent versions of the CPA.[22,27] Comparing all of those calculations with the results shown in Fig. 8, it is seen that there is general agreement that maximum energy of mixing given by the KKR-CPA is smaller than experiment by about 2 mRy for these alloys. The polymorphous CPA calculations of Abrikosov *et al.*[27] give an energy of mixing that is about 1 mRy smaller than experiment, which is in agreement with the LSMS calculations in this paper. Like the present authors, they ascribed the missing 1 mRy to short-range order. The energies of mixing given by the cc-CPA and SCPA calculations of Johnson and Pinski[22] are essentially the same, and that result agrees with experiment without invoking short-range order.

It should be borne in mind that approximations were made in all of these calculations that have nothing to do with the DFT-LDA or with alloy theory. The calculations in this paper employed the muffin-tin approximation, while those in Ref. 22 use the atomic sphere approximation (ASA), and the authors of Ref. 27 employed a tight-binding linear muffin-tin orbital basis in conjunction with an ASA. The LSMS code can be run in a muffin-tin mode or an ASA mode with the flip of a switch. Our experience is that an ASA calculation will give a value for the cohesive energy of a given transition metal system that is 20–30 mRy lower than the muffin-tin value in a multiple-scattering formalism that is otherwise the same. For example, the cohesive energies calculated with the muffin-tin and ASA approximations are $-3275.766\,09$ and $-3275.786\,27$ Ry for fcc Cu with $a=6.7677$ bohr radii, $-3553.144\,45$ and $-3553.165\,22$ Ry for fcc Zn with $a=7.2744$ bohr radii, and $-3275.764\,64$ and $-3275.7843\,47$ Ry for bcc Cu with $a=5.5$ bohr radii. Larger differences have been observed in calculations on the nickel aluminides. To illustrate the extent of these differences, these data show that the difference between the cohesive energies for fcc and bcc Cu is only 1–2 mRy when the atomic volumes are approximately the same. The difference in the cohesive energies predicted by muffin-tin and full-potential calculations is still not known exactly, but all the evidence is that it will be an order of magnitude smaller than the difference between the muffin-tin and ASA energies,[38] particularly for Cu and Zn.

This is not to say that the error in the energy of mixing has the magnitude of the differences discussed above since, as shown in Eq. (3) that energy is a difference between the cohesive energies and a straight line extrapolation between the energies of the pure metals. The fcc Cu and Zn cohesive energies quoted above are the ones used in obtaining the energies of mixing in Fig. 8, and it can be seen that the shifts for the pure metals are almost the same. At the same time, comparisons are not very meaningful in the mRy range until all of the calculations are carried out with the same full-potential methods. The full-potential version of the multiple-scattering method is understood in principle, but it has not yet been fully implemented in the LSMS codes.

It is easy to say that the successes of the isomorphous CPA's are due to a cancellation of errors. There is probably more to it than that, and it would be worth the effort to try to understand the reason theoretically. Although it is now possible to calculate many properties of alloys more or less directly using order-N methods of the type discussed in this paper, there are many good reasons for developing less computationally demanding theories that contain the essential physics. Such theories promote the understanding of the phenomenon, and they can be used to treat a multitude of systems rather than just a few examples. The order-N approach is a useful tool for evaluating approximations used to extend the CPA, as has been demonstrated by the results in this paper.

ACKNOWLEDGMENTS

This work was supported in part by Office of Basic Energy Sciences, Division of Materials Science and Office of Computational and Technology Research, Mathematics, Information and Computational Sciences Division, U.S. Department of Energy, under Subcontract No. DE-AC05-96OR22464 with Lockheed-Martin Energy Research Corporation. We made use of the Intel Paragon XP/S-150 massively parallel supercomputer at the Oak Ridge National Laboratory.

[1] H. M. James and A. S. Ginzbarg, J. Phys. Chem. **57**, 840 (1953), P. Dean, Proc. R. Soc. London, Ser. A **254**, 507 (1960).

[2] R. Alben, M. Blume, H. Krakauer, and L. Schwartz, Phys. Rev. B **12**, 4090 (1975): R. Alben, M. Blume, and M. Mckeown, *ibid.* **16**, 3829 (1977).

[3] I. M. Lifschitz, Zh. Eksp. Teor. Fiz. **44**, 1723 (1963) [Sov. Phys. JETP **17**, 1159 (1963)].

[4] W. Kohn and L. J. Sham, Phys. Rev. A **140**, 1133 (1965).

[5] F. H. Herbstein, B. S. Borie, Jr., and B. L. Averbach, Acta Crystallogr. **9**, 466 (1956); *X-Ray Diffraction*, edited by B. E. Warren (Addison-Wesley, New York, 1969); *Theory of X-Ray and Thermal-Neutron Scattering*, edited by M. A. Krivoglaz (Plenum, New York, 1969).

[6] D. I. Vadets, V. A. Val'chikovskaya, S. E. Naminskaya, and Yu.

I. Perel', Zh. Eksp. Teor. Fiz. **12**, 158 (1973) [Sov. Phys. JETP **16**, 1769 (1973)].
[7] X. Jiang, G. E. Ice, C. J. Sparks, L. Robertson, and P. Zschack, Phys. Rev. B **54**, 3211 (1996).
[8] J. S. Faulkner, Phys. Rev. B **56**, 2299 (1997).
[9] N. F. Mott and H. Jones, *The Theory of the Properties of Metals and Alloys* (Dover, New York, 1958).
[10] L. Nordheim, Ann. Phys. (Leipzig) **9**, 607 (1931); T. Muto, Sci. Papers Inst. Phys. Chem. Research (Tokyo) **34**, 377 (1938).
[11] J. Korringa, J. Chem. Phys. Solids **7**, 252 (1958).
[12] P. Soven, Phys. Rev. **156**, 809 (1967); **178**, 1136 (1969).
[13] J. S. Faulkner, Prog. Mater. Sci. **27**, 1 (1982).
[14] J. R. Klauder, Ann. Phys. (Leipzig) **14**, 43 (1961); R. J. Elliott, J. A. Krumhansl, and P. L. Leath, Rev. Mod. Phys. **46**, 465 (1974); R. Mills and P. Ratanavararaksa, Phys. Rev. B **18**, 5291 (1978).
[15] J. S. Faulkner and G. M. Stocks, Phys. Rev. B **21**, 3222 (1980).
[16] H. Winter and G. M. Stocks, Phys. Rev. B **27**, 882 (1983).
[17] D. D. Johnson, D. M. Nicholson, F. J. Pinski, B. L. Gyorffy, and G. M. Stocks, Phys. Rev. Lett. **56**, 2088 (1986), D. D. Johnson, D. M. Nicholson, F. J. Pinski, B. L. Gyorffy, and G. M. Stocks, Phys. Rev. B **41**, 9701 (1990).
[18] B. L. Gyorffy, D. D. Johnson, F. J. Pinski, D. M. Nicholson, and G. M. Stocks in *Alloy Phase Stability*, Vol. 163 of *NATO ASI Series E: Applied Sciences*, edited by G. M. Stocks and A. Gonis (Kluwer, Dordrecht, 1989).
[19] R. Magri, S. H. Wei, and A. Zunger, Phys. Rev. B **42**, 11 388 (1990).
[20] Z. W. Lu, S.-H. Wei, A. Zunger, S. Frota-Pessoa, and L. G. Ferreira, Phys. Rev. B **44**, 512 (1991); C. Wolverton and A. Zunger, *ibid.* **51**, 6876 (1995); C. Wolverton, A. Zunger, S. Froyen, and S.-H. Wei, *ibid.* **54**, 7843 (1996).
[21] I. A. Abrikosov, Yu. H. Vekilov, and A. V. Ruban, Phys. Lett. A **154**, 407 (1991); I. A. Abrikosov, Yu. H. Vekilov, P. A. Korzhavyi, A. V. Ruban, and L. E. Shilkrot, Solid State Commun. **83**, 867 (1992).
[22] D. D. Johnson and F. J. Pinski, Phys. Rev. B **48**, 11 553 (1993).
[23] P. A. Korzhavyi, A. V. Ruban, I. A. Abrikosov, and H. L. Skriver, Phys. Rev. B **51**, 5773 (1995).
[24] J. S. Faulkner, Yang Wang, and G. M. Stocks, in *Alloy Modeling and Design*, edited by G. M. Stocks, C. T. Liu, and P. E. A. Turchi (The Minerals, Metals, and Materials Society, Warrendale, PA, 1995); J. S. Faulkner, Yang Wang, and G. M. Stocks, *Stability of Materials*, Vol. 355 of *NATO ASI Series B: Physics*, edited by A. Gonis, P. E. A. Turchi, and J. Kudrnovsky (Plenum, New York, 1996), J. S. Faulkner, Yang Wang, Nassrin Moghadam, and G. M. Stocks, in *Proceedings of the First International Alloy Conference (IAC-1)*, edited by A. Gonis, A. Meike, and P. E. A. Turchi (Plenum, New York, 1996).
[25] J. S. Faulkner, Yang Wang, and G. M. Stocks, Phys. Rev. B **52**, 17 106 (1995).
[26] J. S. Faulkner, Yang Wang, and G. M. Stocks, Phys. Rev. B **55**, 7492 (1997).
[27] I. A. Abrikosov, A. M. N. Niklasson, S. I. Simak, B. Johansson, A. V. Ruban, and H. L. Skriver, Phys. Rev. Lett. **76**, 4203 (1996).
[28] G. M. Stocks, D. M. C. Nicholson, Y. Wang, W. A. Shelton, Z. Szotek, and W. M. Temmermann, in *High Performance Computing Symposium; Grand Challenges in Computer Simulation*, Proceedings of the 1994 Simulation Multiconference, edited by A. M. Tentner (The Society for Computer Simulation, San Diego, 1994); D. M. C. Nicholson, G. M. Stocks, Y. Wang, W. A. Shelton, Z. Szotek, and W. M. Temmermann Phys. Rev. B **50**, 14 686 (1994).
[29] Yang Wang, G. M. Stocks, W. A. Shelton, D. M. C. Nicholson, Z. Szotek, and W. M. Temmerman, Phys. Rev. Lett. **75**, 2867 (1995).
[30] Lord Rayleigh, Philos. Mag. **34**, 481 (1892).
[31] J. Korringa, Physica (Amsterdam) **13**, 392 (1947); W. Kohn and N. Rostoker, Phys. Rev. **94**, 111 (1954).
[32] William Hume-Rothery, R. E. Smallman, and C. W. Haworth, *The Structure of Metals and Alloys* (Institute of Metals, London, 1969).
[33] V. L. Moruzzi, J. F. Janak, and A. R. Williams, *Calculated Electronic Properties of Metals* (Pergamon, New York 1978).
[34] W. B. Pearson, *The Crystal Chemistry and Physics of Metals and Alloys* (Wiley-Interscience, New York, 1972).
[35] R. Hultgren *et al.*, *Selected Values of the Thermodynamic Properties of Binary Alloys* (American Society of Metals, Metals Park, OH, 1973).
[36] G. Malcolm Stocks, Bull. Am. Phys. Soc. **42**, 684 (1997).
[37] L. Reinhard, B. Schönfeld, G. Kostorz, and W. Bührer, Phys. Rev. B **41**, 1727 (1990).
[38] G. S. Painter, J. S. Faulkner, and G. M. Stocks, Phys. Rev. B **9**, 2448 (1974); D. M. Nicholson and J. S. Faulkner, Phys. Rev. B **39**, 8187 (1989); A. Gonis, X.-G. Zhang, and D. M. Nicholson, *ibid.* **40**, 947 (1989).